Dynamical properties of the spin-Peierls compound α'-NaV_2O_5

D. Augier[a], D. Poilblanc[a], S. Haas[b], A. Delia[c] and E. Dagotto[c]
(a) Laboratoire de Physique Quantique & Unité Mixte de Recherche CNRS 5626
Université Paul Sabatier, 31062 Toulouse, France
(b) Theoretische Physik, ETH Hönggerberg, 8093 Zürich, Switzerland
(c) Department of Physics and NHMFL, Florida State University, Tallahassee, Florida 32306, USA
(April 97)

Dynamical properties of the novel inorganic spin-Peierls compound α'-NaV_2O_5 are investigated using a one-dimensional dimerized Heisenberg model. By exact diagonalizations of chains with up to 28 sites, supplemented by a finite-size scaling analysis, the dimerization parameter δ is determined by requiring that the model reproduces the experimentally observed spin gap Δ. The dynamical and static spin structure factors are calculated. As for $CuGeO_3$, the existence of a low energy magnon branch separated from the continuum is predicted. The present calculations also suggest that a large magnetic Raman scattering intensity should appear above an energy threshold of 1.9 Δ. The predicted photoemission spectrum is qualitatively similar to results for an undimerized chain due to the presence of sizable short-range antiferromagnetic correlations.

PACS numbers: 64.70.Kb, 71.27.+a, 75.10.Jm, 75.40.Mg, 75.50.Ee

Recently, the quasi-one-dimensional (1D) compound α'-NaV_2O_5 has received considerable attention since it appears to be the second inorganic material showing a spin-Peierls (SP) phase — the first one being $CuGeO_3$ [1]. Below a transition temperature T_{SP}, the compound undergoes a lattice distortion with the opening of a spin gap. The structure of NaV_2O_5 is made of quasi-two dimensional layers of VO_5 square pyramids separated by Na-ions [2]. Two types of VO_5 chains alternate : $V^{4+}O_5^{2-}$ and $V^{5+}O_5^{2-}$ (V^{4+} carries a spin $\frac{1}{2}$ while V^{5+} does not). NaV_2O_5 is a good candidate for a 1D magnetic system since the magnetic $V^{4+}O_5^{2-}$ chains are isolated by non magnetic $V^{5+}O_5^{2-}$ 1D structures.

Originally, the presence of the SP phase transition was suggested by experiments on polycrystalline samples [3,4] which showed a rapid reduction of the magnetic susceptibility below $T_{SP} \simeq 34$ K. From the dependence on the orientation of the magnetic field, recent magnetic susceptibility measurements on single crystals unambiguously established the nature of the low-temperature phase which is a spin symmetric singlet ground state [5]. The observation of structural distortions by X-ray diffraction [6], NMR [4] and Raman scattering [5] further suggested that an underlying spin-phonon coupling is responsible for the SP transition. Note also that the critical temperature T_{SP} is the highest of all known organic or inorganic SP compounds (e.g., $T_{SP}(CuGeO_3) \simeq 14$ K).

The magnetic susceptibility $\chi(T)$ in the high-temperature phase above T_{SP} of this compound seems well-described by a 1D antiferromagnetic (AF) Heisenberg model [3,7]. Indeed, the crystallographic structure of this material suggests that the magnetic frustration is very small. Fits of $\chi(T)$ below T_{SP} provide estimates of both the nearest-neighbor spin exchange J and of the spin gap Δ. Recent measurements on single crystals [5] led to $J = 441$ K and $\Delta \simeq 85$ K in good agreement with previous estimates of J [3,7] and Δ [4,6]. Then, in our analysis below a ratio $\Delta/J = 0.193$ is assumed.

Following the approach used for the SP compound $CuGeO_3$, we will consider here a spin-1/2 AF Heisenberg model with an explicit dimerization of the exchange coupling to account for the lattice distortion,

$$H = J \sum_i (1 + \delta(-1)^i)\, \vec{S}_i \cdot \vec{S}_{i+1} \; . \qquad (1)$$

Note that in the case of $CuGeO_3$ an additional frustration was needed to describe the compound [8,9]. The interchain couplings, although crucial to obtain a finite ordering temperature, are expected to be small and will be neglected here.

The model Eq.(1) has a non-zero spin gap for all $\delta > 0$, and first we will determine the value of δ that reproduces the experimentally measured spin gap. The extrapolation to an infinite chain $L \to \infty$ is performed accurately using the scaling law $\Delta(L) = \Delta + \frac{A}{L}\exp(-\frac{L}{L_0})$ [10]. The presence of a spin gap induces a length scale L_0 and finite size effects are negligible when $L \gg L_0$. As observed in Fig. 1(a) for $\delta = 0.05$, this scaling behavior is indeed accurately satisfied. In addition, for such parameters we have found $L_0 \approx 18$ lattice spacing and, thus, extrapolations using data for systems with up to 28 sites are expected to have small error bars. The behavior of the spin gap as a function of δ is shown in Fig. 1(b). A comparison with the experimental value $\Delta/J = 0.193$ gives an estimate $\delta \simeq 0.048$ for the actual NaV_2O_5 compound to be compared with $\delta \simeq 0.014$ obtained for $CuGeO_3$ [8]. It is interesting to notice that the dimerization is larger for NaV_2O_5, although the ratios

Δ/J are quite similar in both systems [11]. The reason is that, in contrast to NaV_2O_5, a large frustration exists in $CuGeO_3$ from a sizable next-nearest neighbor coupling constant J'. The frustration J' alone can produce a gap when the ratio $\alpha = J'/J$ is larger than $\alpha_c \simeq 0.2411$. For $CuGeO_3$ $\alpha \simeq 0.36$ was proposed [8], while here $\alpha = 0$ is assumed [12].

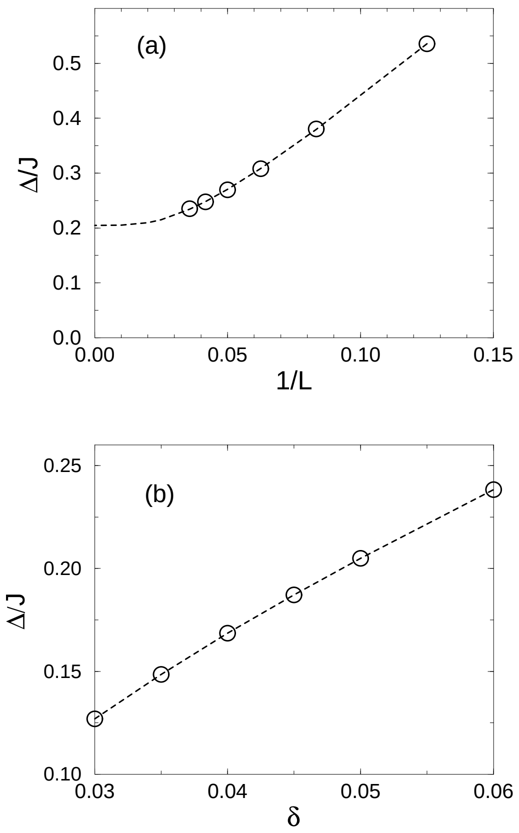

FIG. 1. (a) Spin gap $\Delta(L)$ in units of J for $\delta = 0.05$, as a function of $1/L$. The dashed line is the fitting curve described in the text. (b) Bulk extrapolated value of Δ/J vs δ.

Let us now proceed with the study of some dynamical properties of NaV_2O_5. Typically, there are a number of experiments giving access to frequency dependent spectral functions of the form

$$I_A(\omega) = -\frac{1}{\pi} \lim_{\varepsilon\to 0} \Im m \, \langle \Psi_0 | A \frac{1}{\omega + i\varepsilon - H + E_0} A^\dagger | \Psi_0 \rangle, \quad (2)$$

where Ψ_0 is the ground state, E_0 its energy, and A is some operator describing the physical process under consideration. Using exact diagonalization (ED) techniques, $I_A(\omega)$ can be calculated with a continued fraction expansion [13]. An imaginary component $i\varepsilon$ is added to ω in Eq.(2) providing a small width to the δ-functions.

In particular, inelastic neutron scattering (INS) is an accurate momentum dependent probe of the spin dynamics. Based on our model Eq.(1) and the parameter δ calculated here, we can predict the dynamical spin structure factor $S_{zz}(q,\omega)$ measured by INS. $S_{zz}(q,\omega)$ is given by Eq.(2) with $A = S_z(q)$ and $S_z(q) = 1/\sqrt{L}\sum_j \exp(iqr_j)S_z(j)$. The results on a 28 site chain are shown in Fig. 2 for all momenta $q = n\frac{\pi}{14}$, $n = 0, \cdots, 14$. We clearly observe a well-defined q-dependent low energy feature of bandwidth $\sim 1.6\ J$ having the largest weight located around $q = \pi$. This is certainly reminiscent of the Des Cloiseaux-Pearson [14] (DP) excitation spectrum of the Heisenberg chain. However, important differences arise from the presence of dimerization : (i) because of the spin gap there is no intensity for $\omega < \Delta$ at $q = 0$ and $q = \pi$; (ii) the lowest singlet-triplet excitation branch which has been interpreted as a spinon-spinon bound state [15] is well separated from the continuum by a second gap.

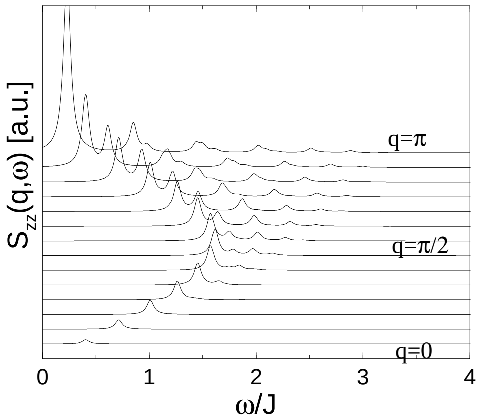

FIG. 2. Spectral function $S_{zz}(q,\omega)$ calculated at momenta $q = \frac{2\pi n}{L}$ ($L = 28$ and $\delta = 0.048$) and using a small broadening $\varepsilon = 0.04J$. From bottom to top, n moves from 0 to 14.

The dispersion relation of the lowest energy magnon branch is presented in Fig. 3 with an infinite size extrapolation for momenta $q = \pi/2$ and $q = \pi$ (spin gap). The finite size effects are quite small, especially for $q = \pi/2$. The second peak, as well as the upper limit of the continuum of excitations, are also shown. The dispersions of the lowest excitations are symmetric with respect to $\pi/2$, reflecting the doubling of the unit cell by dimerization. However, note that the spectral weight is *not* symmetric. As observed in Fig. 3, we have also explicitly checked at $q = \pi/2$ that the magnon excitation is separated from the continuum by a gap.

The static structure factor $S_{zz}(q) = \int d\omega\, S_{zz}(q,\omega)$ and the weight of the first peak are shown in Fig. 4. $S_{zz}(q)$ is sharply peaked at $q = \pi$ due to strong short-range AF correlations. A sizable fraction of the weight is located above the magnon branch, specially at intermediate momenta such as $q \simeq 5\pi/7$ where the continuum should be better observed experimentally.

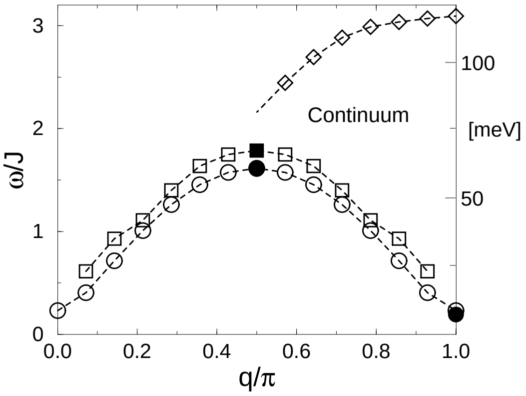

FIG. 3. Momentum dependence of the first (∘), second peak (□) and the upper limit for the continuum (⋄) excitations ($L = 28$ and $\delta = 0.048$). The extrapolations to infinite size are also shown for $q = \pi/2$ (■, •) and $q = \pi$ (•). Units on the right are meV (assuming $J = 440\ K$).

It is interesting to make a quantitative comparison with $CuGeO_3$. Assuming $J = 440K$, Fig. 3 shows that the maximum of the magnon branch occurs around $\omega_{max} \simeq 60$ meV while the spin gap is of order $\Delta \simeq 7.3$ meV. Thus, the energy scales are approximately 4 times larger than for $CuGeO_3$ [16,17] which might restrict the INS experiments to the bottom of the spectrum around $q = \pi$ [6]. Also, we observed that the ratio ω_{max}/J is close to the DP value of 1.57, while in $CuGeO_3$ it is approximately 1.2 [17,18]. This is due to the fact that the large frustration J' in $CuGeO_3$ affects the entire excitation spectrum, while in NaV_2O_5 only the low energy part of the spectrum is modified by the small dimerization. The ratio ω_{max}/J is then a key quantity to confirm experimentally the absence of frustration in this system using INS. In addition to the change in the value of ω_{max}/J, frustration would also lead to a qualitatively different global structure of the spectrum. As example, the upper limit of the continuum should be better defined for $CuGeO_3$ ($J' \neq 0$) than for NaV_2O_5 ($J' = 0$).

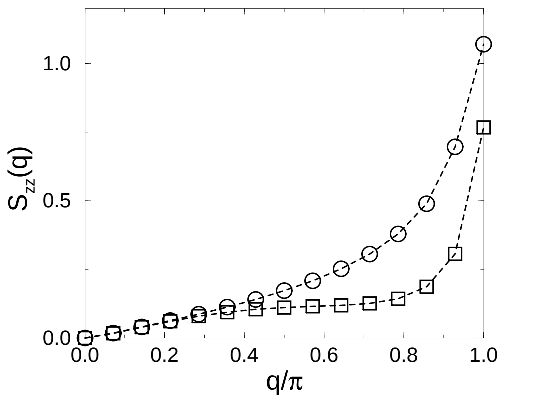

FIG. 4. Static structure factor $S_{zz}(q)$ (∘) and weight of the first excitation (□) as a function of q ($L = 28$ and $\delta = 0.048$).

Raman scattering is another powerful technique to probe the spin dynamics. The effective Hamiltonian for the photon-spin interaction is given by [19]

$$H_{\text{eff}} = g \sum_{<ij>} (\vec{e}_{in}.\vec{R}_{ij})(\vec{e}_{out}.\vec{R}_{ij})\vec{S}_i.\vec{S}_j \ . \tag{3}$$

$\vec{e}_{in}$ ($\vec{e}_{out}$) is the polarisation vector of the incoming (outgoing) photons, the sum is over nearest-neighbor spins, $\vec{R}_{ij}$ is the vector connecting them, and g is a coupling constant that depends on the incoming photon frequency. H_{eff} is a spin-singlet, translationally invariant operator, and it corresponds to physical processes involving the simultaneous excitations of two magnons with opposite momenta. Since the small interchain coupling has been neglected, $\vec{R}_{ij}$ has to be collinear to the chain. The largest Raman scattering intensity is thus expected for a polarisation of both photons along the chain direction. The Raman operator can then be written [10,20] (taking $g = 1$) as $H_R = \sum_i (-1)^i \vec{S}_i \cdot \vec{S}_{i+1}$. The Raman intensity $I_R(\omega)$ (Fig. 5) reveals a large scattering band centered at a mean energy (defined as the first moment of the spectrum $\langle\omega\rangle = \int d\omega\omega I_R(\omega) / \int d\omega I_R(\omega)$) of $\sim 2.9J$. $I_R(\omega)$ is fairly smooth (the oscillations at low energy are finite size effects) and no Van Hove singularity is observed at the energy 2 ω_{max}, associated with the top of the magnon branch. Due to the spin gap, an energy threshold Δ' appears in the Raman scattering spectrum. The infinite size extrapolation of the corresponding singlet-singlet gap gives $\Delta' \simeq 0.37J$ as indicated in Fig. 5. The ratio of the singlet-singlet gap over the singlet-triplet gap is equal to $\Delta'/\Delta \simeq 1.9$ close to the prediction of $\sqrt{3}$ [15]. Since we probe here double magnon excitations this suggests that magnons are almost non-interacting bosonic excitations (which would give $\Delta'/\Delta = 2$ exactly).

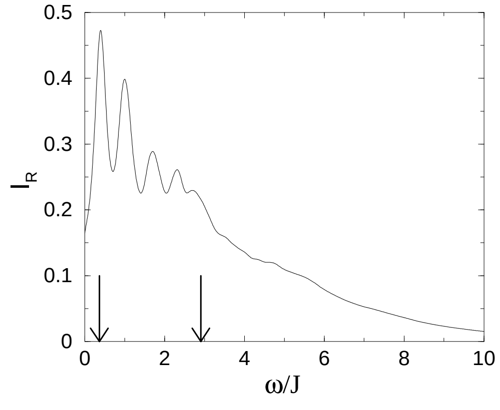

FIG. 5. Raman intensity for $L = 28$ and $\delta = 0.048$. A broadening $\varepsilon = 0.2J$ was used. The arrows indicate the extrapolated singlet-singlet gap Δ' at low energy and the first moment of the distribution $\langle\omega\rangle$ at higher energy.

We end our study of dynamical properties of NaV_2O_5 with an investigation of the angle resolved photoemission spectrum (ARPES). In this case the relevant operator A in Eq.(2) is the destruction operator $c_{p\sigma}$ of an electron with momentum p and spin σ. Results will be presented for two hole hopping amplitudes, i.e. $t = J$ and $t = 2.5\,J$, since it is *a priori* difficult to anticipate its actual value.

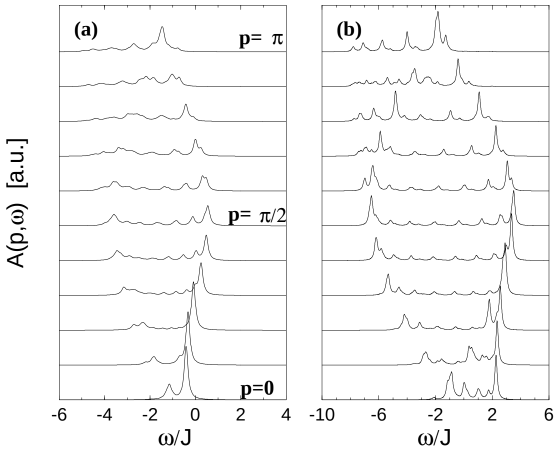

FIG. 6. Hole spectral function $A(p,\omega)$ on a chain of 20 sites for $t/J = 1$ (a) and $t/J = 2.5$ (b) and broadening $\varepsilon = 0.1J$. From bottom to top the momentum varies from 0 to π.

The results shown in Fig. 6 are very similar to the case of a single hole in a half-filled infinite-U Hubbard model [21] or in the frustrated Heisenberg chain [16]. The overall scale of the spectrum is clearly given by t. For $p < \pi/2$ a holon and spinon branches appear, while a "shadow band" is observed for $p > \pi/2$ caused by short-range magnetic scattering at $q = \pi$ [16]. Above the continuum, the high energy structure can be associated with a reflection of the shadow band at the zone boundary [21]. However, note that the presence of a spin gap introduces some subtle differences with predictions for undimerized systems that could be detected in ARPES experiments. For instance, doping a spin gap insulator leads in general to a metallic state with only one zero-energy mode [22] (corresponding to collective *charge* excitations only). This is reflected in Fig. 6 by the fact that the so-called spinon branch is in fact a broad structure instead of a branch-cut. In addition, the small peak at very low energy just above $k_F = \pi/2$ might be associated to a holon-spinon bound state. Similar results were obtained for $CuGeO_3$ [16]. In spite of these subtleties, it is clear that the spectral function of the dimerized model Eq.(1) has strong similarities with undimerized systems. The main reason is that here an explicit dimerization coexists with sizable short-range AF correlations, a detail not sufficiently remarked in the literature on the subject.

In conclusion, using recent experimental data on the SP NaV_2O_5 system, the magnitude of the dimerization of the AF exchange coupling along the chain has been determined. In the framework of a 1D dimerized Heisenberg model, several theoretical predictions for INS, Raman double magnon scattering, and ARPES were here presented. Our calculations are expected to provide theoretical guidance for future experiments on SP systems.

We thank IDRIS (Orsay) for allocation of CPU time on the C94 and C98 CRAY supercomputers. E. D. is supported by grant NSF-DMR-9520776 and S. H. by the Swiss National Science Foundation.

---

[1] M. Hase, I. Terasaki, and K. Uchinokura, Phys. Rev. Lett. **70**, 3651 (1993).
[2] M. Pouchard, A. Casalot, J. Galy and P. Hagemuller, Bull. Soc. Chim. Fr. **11**, 4343 (1967); see also A. Carpy and J. Galy, Acta Crystallogr. Sect. **B31**, 1481 (1975).
[3] M. Isobe and Y. Ueda, J. Phys. Soc. Jpn. **65**, 1178 (1996).
[4] T. Ohama et al., J. Phys. Soc. Jpn. **66**, 545 (1997).
[5] M. Weiden, R. Hauptmann, C. Geibel, F. Steglich, M. Fischer, P. Lemmens and G. Güntherodt, preprint cond-mat/9703052.
[6] Y. Fujii et al., J. Phys. Soc. Jpn. **66**, 326 (1997).
[7] F. Mila, P. Millet and J. Bonvoisin, Phys. Rev. B **54**, 11 925 (1996).
[8] J. Riera and A. Dobry, Phys. Rev. B **51**, 16098 (1995).
[9] G. Castilla, S. Chakravarty and V. J. Emery, Phys. Rev. Lett. **75**, 1823 (1995).
[10] G. Bouzerar, A. P. Kampf and F. Schönfeld, preprint cond-mat/9701176.
[11] The *absolute* value of the spin gap of $CuGeO_3$ is in fact much smaller than the one of NaV_2O_5 due to a large difference between the exchange couplings.
[12] Note however that a small frustration has only little effects on the value of δ at constant spin gap (e.g. a frustration $\alpha = 0.05$ gives $\delta = 0.044$ to be compared to $\delta = 0.048$ without frustration).
[13] For a review on ED see e.g. D. Poilblanc in *Numerical Methods for Strongly Correlated Systems*, edited by D. J. Scalapino (Frontiers in Physics, 1997). See also E. Dagotto, Rev. Mod. Phys. **66**, 763 (1994).
[14] J. Des Cloiseaux and J. J. Pearson, Phys. Rev. **128**, 2131 (1962).
[15] G. S. Uhrig and H. J. Schulz, Phys. Rev. B **54**, R9624 (1996).
[16] S. Haas and E. Dagotto, Phys. Rev. B **52**, R14396 (1995).
[17] D. Poilblanc, J. Riera, C. A. Hayward, C. Berthier and M. Hortavić, Phys. Rev. B **55**, Rxxx, (May, 1997) ; A. Fledderjohann and C. Gros, Europhys. Lett. **37**, 189 (1997).
[18] L. P. Regnault et al., Phys. Rev. B **53**, 5579 (1996).
[19] P. A. Fleury and R. Loudon, Phys. Rev. **166**, 514 (1968).
[20] V.N. Muthukumar et al., Phys. Rev. B **54**, R9635 (1996).
[21] S. Sorella and A. Parolla, J. Phys. Cond. Matter **4**, 3589 (1992). See also K. Penc et al., Phys. Rev. Lett. **77**, 1390 (1996); J. Favand et al., Phys. Rev. B **55**, R4859 (1997).
[22] The doped spin ladder system is a prototype of such a system. For a review see e.g. E. Dagotto and T. M. Rice, Science **671**, 619 (1996); see also C. Hayward and D. Poilblanc, Phys. Rev. B **53**, 11721 (1996).